

Article

Thermoactivated Dislocation Motion in Rolled and Extruded Magnesium: Data of the Low-Temperature Acoustic Experiment

Pavel Pal-Val ^{1,*}, Olena Vatazhuk ¹, Andriy Ostapovets ^{2,*} , Lubomír Král ² and Jan Pinc ³ 

¹ B. Verkin Institute for Low Temperature Physics and Engineering of NAS of Ukraine, 47 Nauky Ave., 61103 Kharkiv, Ukraine; vatazhuk@ilt.kharkov.ua

² Institute of Physics of Materials, Czech Academy of Sciences, Žižkova 22, 61600 Brno, Czech Republic; lkral@ipm.cz

³ Institute of Physics, Czech Academy of Sciences, Na Slovance 2, 18221 Prague, Czech Republic; pinc@fzu.cz

* Correspondence: palval@ilt.kharkov.ua (P.P.-V.); ostapov@ipm.cz (A.O.)

Abstract: Acoustic properties (logarithmic decrement and dynamic Young's modulus) of commercial grade magnesium have been measured in the temperature range 51–310 K. Two types of magnesium samples have been studied: polycrystalline magnesium rolled at room temperature and subjected to hot extrusion. It is shown that the amplitude dependences of the acoustic properties are due to the thermally activated breakaway of dislocations from weak pinning centers. Within the framework of the Indenbom-Chernov theory of thermally activated dislocation hysteresis, the binding energy of the interaction between dislocations and defects was estimated. Furthermore, dependences of the activation energy and activation volume on the applied stress were obtained in the microplastic region. The temperature dependences of the dynamic Young's modulus are obtained in the amplitude independent region in the temperature range of 51–310 K. Functional form of the Young's modulus temperature dependences corresponds to the classical concepts of the effect of thermal excitation of electrons and phonons on the elastic properties of crystals.

Keywords: HCP metals; magnesium; dislocations; acoustic properties; low temperatures



Citation: Pal-Val, P.; Vatazhuk, O.; Ostapovets, A.; Král, L.; Pinc, J. Thermoactivated Dislocation Motion in Rolled and Extruded Magnesium: Data of the Low-Temperature Acoustic Experiment. *Metals* **2021**, *11*, 1647. <https://doi.org/10.3390/met11101647>

Academic Editor: Qingping Cao

Received: 3 September 2021

Accepted: 14 October 2021

Published: 18 October 2021

Publisher's Note: MDPI stays neutral with regard to jurisdictional claims in published maps and institutional affiliations.



Copyright: © 2021 by the authors. Licensee MDPI, Basel, Switzerland. This article is an open access article distributed under the terms and conditions of the Creative Commons Attribution (CC BY) license (<https://creativecommons.org/licenses/by/4.0/>).

1. Introduction

It is well known that physical and mechanical properties of metals are largely determined by the presence of crystal structure defects (point defects, dislocations, twins, grain boundaries, etc.). The defect structure is formed both during the growth of metal polycrystals and during their further processing using various technological schemes. Plastic deformation is technological method, which is commonly used to obtain the required size and shape. This process leads to formation of a large density of crystal defects, primarily dislocations. Dynamic behavior of crystal structure can be effectively studied by acoustic spectroscopy methods. The presence of dislocations causes a number of linear and nonlinear effects observed during study of the acoustic properties of crystalline solids. Linear dislocation acoustic effects include, as a rule, relaxation peaks in the temperature or frequency dependences of sound absorption, as well as the associated stepwise changes in the elastic moduli of crystals (modulus defects) [1–4]. Nonlinear effects are manifested in a strong dependence of the absorption of the energy of elastic vibrations as well as elastic moduli on the amplitude of alternating deformation ϵ_0 in the crystal [5–10].

A number of microscopic mechanisms have been proposed for description of the dynamic behavior of dislocations in the stress field of a sound wave [11–13] to explain the dislocation acoustic effects. Combined with reliable experimental data on dislocation contributions to sound absorption and modulus defect, these models could, in principle, provide extensive information on the dynamic behavior of dislocations in crystals. This is especially true for amplitude-dependent acoustic effects. However, the relatively small number of reliable experimental results obtained in this area (including at cryogenic temperatures), a

simplified theoretical description, the complexity and variety of real dislocation processes during the excitation of sound (including high-amplitude sound) leads to necessity of further accumulation of new experimental data. The new experimental data together with their phenomenological description will allow creating reliable experimental basis for construction of a more adequate microscopic description of the phenomena under study.

Magnesium and its alloys are currently being intensively studied as promising lightweight materials of low density. They are widely used as structural materials in the aerospace industry. Aircraft components and instrumentation often should operate at low or moderately low temperatures. In contrast to materials with a cubic crystal structure, Mg has several slip systems with very different critical resolved shear stresses. It can lead to competition between different elementary mechanisms of plastic deformation at low temperatures, most of which are thermally activated at moderately low temperatures [14]. Present paper reports dynamic dislocation effects observed in amplitude-independent and amplitude-dependent regions of ultrasonic vibrations in commercially pure magnesium polycrystals subjected to different types of plastic deformation. Two types of plastic deformation are considered: cold rolling and hot extrusion. It is expected that basal slip and deformation twinning are the main plastic mechanisms activated in cold rolling in contrast to hot extrusion, where non-basal slip also plays significant role. Consequently, these two types of treatment result in different level of plastic deformation, different dislocation density as well as in difference in microstructures and textures. Elastic and inelastic properties of magnesium and magnesium alloys have been previously studied mostly in the temperature range near and above room temperature [5–9,14–18]. To fill to some extent this gap, in the present work linear and nonlinear dislocation acoustic effects were studied in the temperature range 51–300 K.

2. Experimental

2.1. Material

Magnesium with a purity of 99.95% was used for sample preparation. Two types of plastic deformation treatment were applied to the as-received material: rolling and hot extrusion. Structure of initial as-cast material is illustrated in Figure 1. Samples for rolling and extrusion were cut from different coarse-grained ingots with grain size of $200 \mu\text{m}^{-1}$ mm. The first series of the sample were obtained by rolling of magnesium ingots at room temperature. The value of the total plastic deformation during rolling was about 20%. To obtain another series of samples, coarse-crystalline magnesium billets with 20 mm in diameter were subjected to hot extrusion process at the temperature of 300 °C with a strain rate of 5 mm/s. The extrusion ratio was of 10 to 1 (20 mm–6 mm).

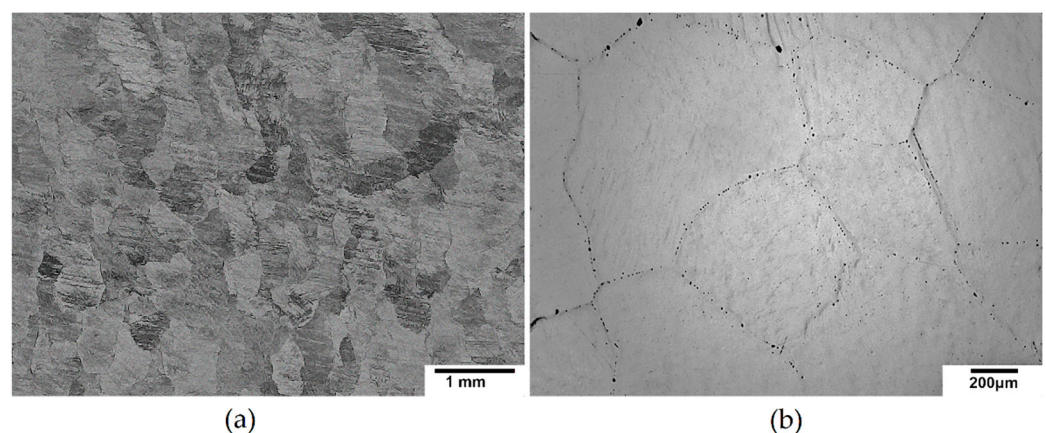


Figure 1. Light micrographs of initial as-cast material used (a) for rolling and (b) for extrusion.

The main characteristics of sample structures were obtained by electron backscatter diffraction (EBSD) using a Tescan LYRA 3 XMU FEG/SEMxFIB electron microscope

equipped with an EBSD Nordlys Nano detector from Oxford Instruments (Figure 2a,b). The sample was metallographically ground using water-lubricated sandpaper (grid up to 2500). After the grinding process, the sample was polished with a 1 μm diamond paste with ethanol as a lubricant. After polishing, the sample was electropolished for 2 min at 20 V in HCl/ethylene glycol electrolyte and at $-10\text{ }^\circ\text{C}$. EBSD analysis of rolled and extruded samples was performed at an accelerating voltage of 20 kV. The analysis was performed at different magnifications due to very different grain sizes of the experimental materials. Therefore, different parameters of the EBSD analysis were chosen. The analysis area of the rolled coarse grain sample was $1.46\text{ mm} \times 1.1\text{ mm}$ and the analysis step was $5\text{ }\mu\text{m}$. The analysis area of the extruded fine-grained sample was $0.146\text{ mm} \times 0.110\text{ mm}$, and the analysis step was $0.4\text{ }\mu\text{m}$.

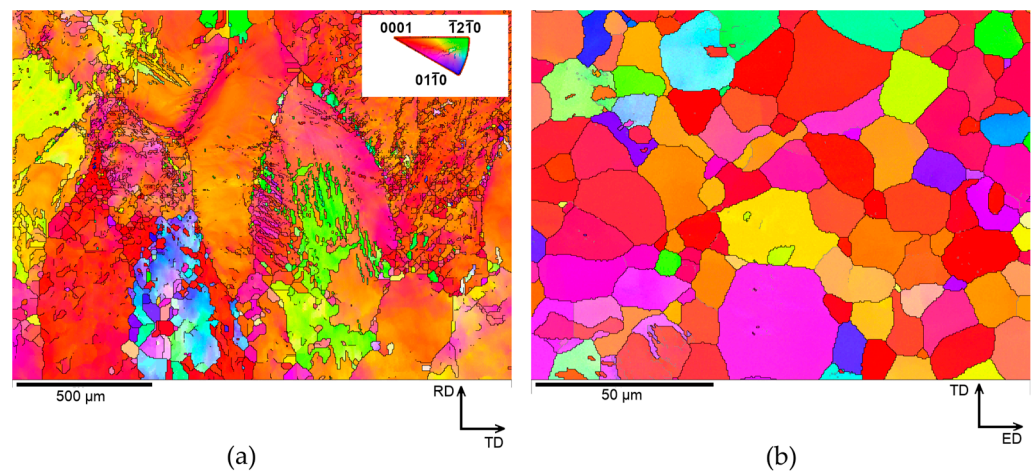


Figure 2. Electron backscattered diffraction (EBSD) maps for (a) rolled (inset—orientation color key) and (b) extruded Mg samples. The maps were collected from RD-TD plane or ED-TD plane in the case of rolling and extrusion, respectively.

The rolled samples demonstrated an extremely inhomogeneous distribution of grain sizes: along with a large number of small grains ($\sim 10\text{ }\mu\text{m}$ and less), a significant number of large grains ($\sim 200\text{ }\mu\text{m}$ or more) were noted in the samples, which, moreover, turned out to be elongated along the rolling direction with the ratio of the longitudinal to transverse dimensions up to 3:1 (see Figures 2a and 3a).

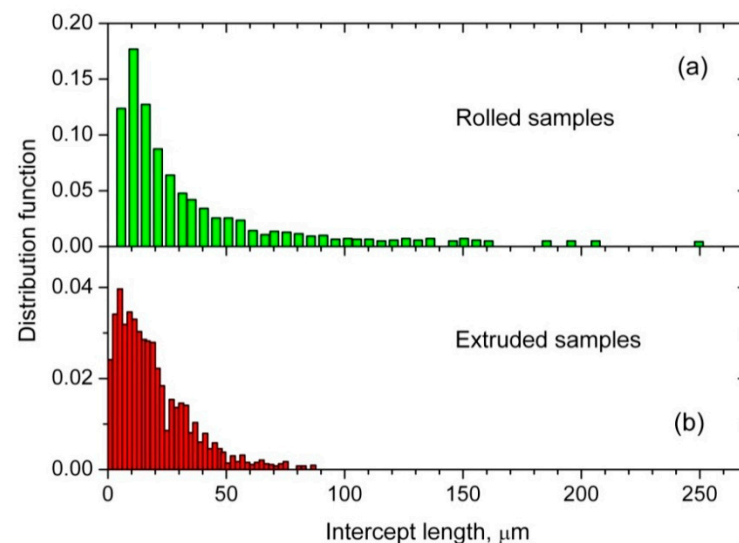


Figure 3. Distribution of grain sizes in (a) rolled and (b) extruded samples.

The extruded samples had a finer-grained structure with a more uniform distribution of grain sizes and a higher degree of their equiaxiality (see Figures 2b and 3b). The average grain sizes in the rolled and extruded samples were 49 μm and 15 μm , respectively. All samples had a noticeable deformation texture. The texture of rolled samples is typical rolling texture for magnesium [19] and can be characterized by basal planes that almost parallel to the rolling (RD-TD) plane (Figure 4a). The texture of extruded samples can be characterized by basal planes parallel to extrusion direction (Figure 4b). Information on the deformation texture in the grain structure of the samples is presented by pole figures (see Figure 4a,b).

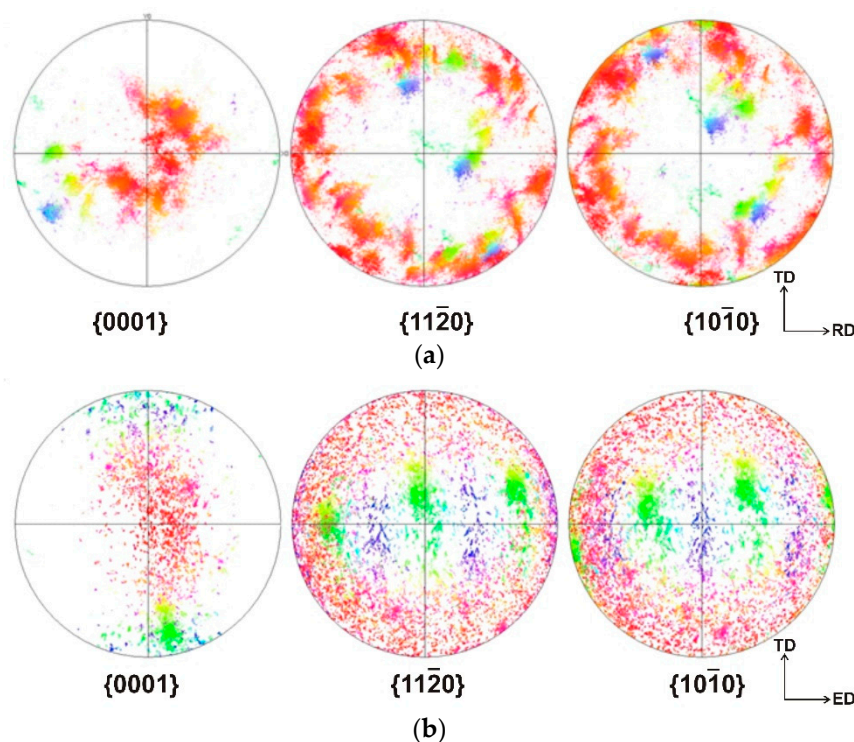


Figure 4. Pole figures of (a) rolled Mg samples (rolling direction RD, right; transverse direction TD, top; normal direction ND, projection plane) and (b) extruded Mg samples (extrusion direction ED, right; transverse direction TD, top; normal direction ND, projection plane).

2.2. Acoustic Measurements

The study of the acoustic properties of Mg in the frequency range 70–350 kHz was carried out by the two-component composite vibrator technique with piezoquartz transducer (details can be found in [20]). Block diagram of the experimental setup is shown in Figure 5.

Longitudinal standing waves were excited in the samples at the fundamental frequency and at the 3rd and 5th harmonics of quartz transducers. Samples for low-temperature acoustic measurements were cut from rolled sheets and extruded rods using electric spark erosion machine and brought to the dimensions required for acoustic measurements using abrasive materials of various fineness. After electrospark cutting of the sample billets, we brought them to the required size using emery paper from the Swiss company SIA (sheets 23 cm \times 28 cm, abrasive 1600 SIANOR, SIA Abrasives Industries AG, Frauenfeld, Switzerland) with a finishing grit size P 1500. The parallelepiped shaped samples were cut with the longest their dimension along either rolling (RD) or extrusion (ED) direction. Correspondingly, the RD and ED were propagation directions of longitudinal acoustic waves with frequency $f \approx 7 \times 10^4 \text{ s}^{-1}$, which were initiated in the sample. It can be concluded from Figure 3 that this direction mainly corresponds to $[10\bar{1}0]$ in the rolled samples. However, there is no preferable crystallographic direction along ED in extruded

samples. The acoustic contact between the transducers and the samples was created using a cyanoacrylic adhesive composition, which endure repeated thermal cycling in the entire investigated temperature range of 51–310 K at thermal cycling rates from 0.01 to 10 K/min. The reproducibility of the results with repeated gluing of samples was close to 100%.

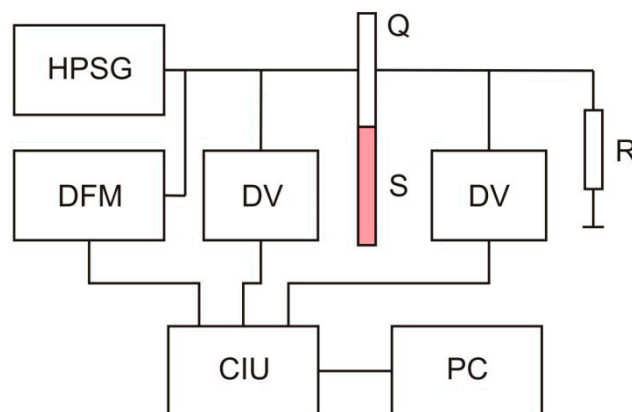


Figure 5. Block diagram of the experimental setup for measuring by the two-component composite vibrator techniques in the ultrasonic frequency range. HPSG is the high precision signal generator; DV are the digital voltmeters; DFM is the digital frequency meter; CIU is the control and interfaces unit; PC is a personal computer; Q is a piezoelectric quartz transducer; S is the sample under study.

Composite vibrators were located inside the evacuated cell placed in a helium cryostat. The main refrigerant was liquid nitrogen. Temperatures 51–77 K were obtained by pumping vapors over the surface of liquid and solidified nitrogen. Intermediate temperatures were obtained using an electrical heater, which was controlled by an automatic temperature control system. The temperature and amplitude dependences of the logarithmic decrement of oscillations $\delta(T, \varepsilon_0)$ and the dynamic Young's modulus $E(T, \varepsilon_0)$ were measured. Amplitude (ε_0) is defined here as amplitude of the longitudinal deformation in an elastic standing wave: $\varepsilon_0 = \sigma_0 / E$ (σ_0 is the stress amplitude; E is the Young's modulus).

3. Results and Discussion

3.1. Amplitude Dependences of Acoustic Properties

The effect of temperature on the parameters of the amplitude-dependent sound absorption and the relative change in the dynamic Young's modulus (modulus defect) was qualitatively similar for all samples studied. The amplitude dependences of the logarithmic decrement and modulus defect are shown in Figure 6a–d for the case of rolled and extruded samples. For clarity, Figure 6a,c show the dependences of the amplitude-dependent part of the decrement $\delta_H(\varepsilon_0, T) = \delta(\varepsilon_0, T) - \delta_i(\varepsilon_0 \rightarrow 0, T)$, i.e., the decrement in the amplitude independent region δ_i was regarded as background decrement and was subtracted from the measured values of δ .

The dependences $\delta_H(\varepsilon_0)$ and $(\Delta E/E)_H(\varepsilon_0)$ had well-defined linear (amplitude independent) and nonlinear (amplitude dependent) regions. An increase in temperature led to a monotonic shift of the critical amplitude of the beginning of the nonlinear section ε_{0c} towards lower values of the deformation amplitudes. Wherein, in the selected semi-logarithmic coordinates, the curves $\delta_H(\varepsilon_0)$ and $(\Delta E/E)_H(\varepsilon_0)$ were shifted almost parallel to themselves. In other words, the shift of the dependences $\delta_H(\varepsilon_0)$ and $(\Delta E/E)_H(\varepsilon_0)$ with a change in temperature was equivalent to a change in the scale along the axis of the deformation amplitudes ε_0 . Such behavior of the amplitude dependences was observed up to a certain crossover temperature T_{co} , which turned out to be different for rolled and extruded samples. In the extruded samples, it was $T_{co} \approx 250$ K, and in the rolled samples $T_{co} \approx 190$ K. Above T_{co} , the curves practically did not shift with temperature, and in some cases their shift towards low temperatures was observed. The amplitude dependences of

the decrement and modulus defect in the extruded samples had a higher steepness and lower values of the critical amplitude ε_{0c} (see Figure 6c,d) than in the rolled samples.

The most probable reasons for the dependence of the logarithmic decrement and the dynamic elastic modulus on the amplitude of ultrasonic vibrations are nonlinear effects associated with the unpinning of dislocations from local pinning centers, e.g., interstitial and substitutional impurities, their clusters, intrinsic interstitial atoms, vacancies, etc. The shift of the $\delta_H(\varepsilon_0)$ and $(\Delta E/E)_H(\varepsilon_0)$ curves with a temperature indicates a thermally activated nature of overcoming local pinning centers by dislocations. The analysis of experimental results shown in Figure 6a,b within the available theoretical concepts allows one to obtain quantitative estimation of the thermoactivation parameters for overcoming weak pinning centers by dislocations.

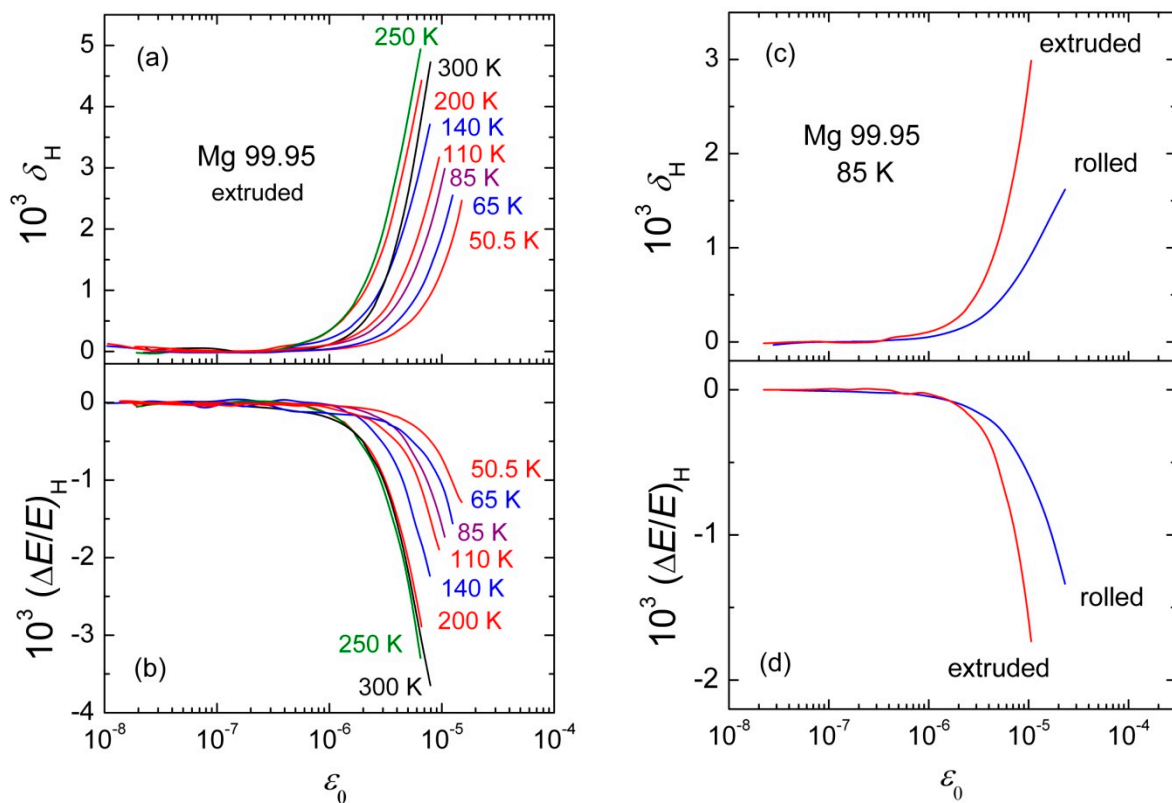


Figure 6. Effect of the temperature (a,b) and deformation mode (c,d) on the amplitude-dependent part of the decrement δ_H and the modulus defect $(\Delta E/E)_H$ in the extruded and rolled samples.

Most theories of amplitude-dependent dislocation absorption of ultrasound are based on the Granato-Lücke hysteresis model [11]. According to this theory, crystalline materials contain a network of dislocations, and the distance L_N between the nodes of the network is postulated to be the same for the entire crystal. It is assumed that the nodes of the net are strong obstacles for dislocations that cannot be overcome when an oscillatory load is applied. Dislocations are randomly pinned between the nodes of the network by point defects. Point defects (impurities, interstitials, vacancies) are weak pinning centers and can be overcome by dislocations in the slip plane under the action of ultrasound. The breakaway of dislocations from weak pinning centers occurs when the amplitude of the applied stress σ_0 exceeds a certain critical stress σ_M of mechanical breakaway of a double dislocation loop from the pinning center:

$$\sigma_M = F_M b L_c, L_c = (l_1 + l_2)/2, \quad (1)$$

where l_1 and l_2 are the lengths of two adjacent segments, b is Burgers' vector of dislocation and F_M is the maximum force of interaction of a dislocation with an impurity. Breakaway even from one weak pinning point in the dislocation line causes a catastrophic breakaway of the entire L_N loop between the nodes. For this type of breakaway of dislocation segments and the exponential distribution of their lengths, the dependence of the amplitude-dependent part of the decrement δ_H on the amplitude of the applied stress was obtained:

$$\delta_H = \frac{C_1}{\sigma_0} \exp\left(-\frac{C_2}{\sigma_0}\right), \quad (2a)$$

where $C_1 = \frac{4\Lambda L_N^3 \sigma_M}{\pi^3 L_c}$, $C_2 = \frac{\pi \sigma_M}{4}$, Λ is the dislocation density and σ_0 is stress amplitude. The C_1 and C_2 values are determined by the parameters of the dislocation structure of a given crystal and can be obtained by rearranging the experimental data in the so-called Granato-Lücke coordinates [11]:

$$\ln(\delta_H \sigma_0) = \ln C_1 - \frac{C_2}{\sigma_0} \quad (2b)$$

Provided that the assumptions made when deriving Equation (2a) are correct, the Granato-Lücke graph should be a straight line that cuts off the value $\ln C_1$ on the ordinate axis and has a slope equal to C_2 .

The initial Granato-Lücke theory considered the breakaway of dislocation segments at $T = 0$ K, i.e., without taking into account the effect of thermal fluctuations. Later the authors of [11] have shown that the effect of thermal activation can be taken into account by simply replacing σ_M in Equation (2a) with the breakaway stress σ_T at a finite temperature [13]:

$$\sigma_T = \sigma_M \psi(T), \quad (3)$$

where in $\psi(T) = 1 - [(kT/U_0) \ln(A)]^{2/3}$; $A = \frac{2}{3} \left(\frac{kT}{U_0}\right)^{2/3} \frac{\nu_0 \sigma_M}{2\pi f \sigma_0}$, k is the Boltzmann constant, U_0 is the binding energy of the dislocation with the pinning center, ν_0 is the attack frequency, f is the frequency of ultrasound.

As a result, for the range of finite temperatures, the following expression was obtained for $\delta_H(T, \sigma_0)$:

$$\delta_H(\sigma_0, T) = C_{1T} \sigma_0 \exp\left(-\frac{C_{2T}}{\sigma_0}\right), \quad (4a)$$

with $C_{1T} = \frac{\Lambda L_N^2 \nu_0}{12\pi U_0 f} \left(\frac{3\pi k T L_c^3}{2G}\right)^{1/2}$, $C_{2T} = \frac{4}{3} \frac{U_0}{kT} \left(\frac{U_0 G}{L_c^2}\right)^{1/2}$. Equation (4a) can also be linearized as follows:

$$\ln \frac{\delta_H}{\sigma_0} = \ln C_{1T} - \frac{C_{2T}}{\sigma_0} \quad (4b)$$

It should be noted that the dimensions C_1 and C_{1T} , as well as C_2 and C_{2T} , are not the same. The experimental data obtained in this work, rearranged according to (2b) and (4b), do not fit into straight lines (see Figure 7), which indicates their inconsistency with the theoretical concepts suggested in [8,11].

Indenbom and Chernov [12] did not use the model of "catastrophic breakaway" of dislocations from weak pinning centers and considered the model of double loop breakaway (the so-called "binding energy" approximation). They have showed that the amplitude-dependent part of the decrement is a function of only one parameter L_{\min} , which is the minimum total length of two adjacent segments, for which the breakaway of a double dislocation loop is possible at a given level of external stress and a given temperature:

$$L_{\min} = F(T)/(b\sigma_0). \quad (5)$$

Here $F(T)$ is the total force of interaction of a dislocation with a local defect at a given temperature. In turn, $F(T)$ is a solution to the equation

$$U(F) = kT \ln\left(\frac{v_0}{f}\right), \tag{6}$$

where U is the activation energy. It was shown in [12] that a change in temperature is equivalent to a change in the amplitude of the applied stress; the curves of the amplitude dependence measured at different temperatures should coincide when appropriately varying the stress-amplitude scale. As can be seen from Figure 8a, the temperature variation is actually equivalent to a stress amplitude variation. Corresponding curves $\delta_H(\varepsilon_0)$ in semilogarithmic co-ordinates differ only by a constant displacement.

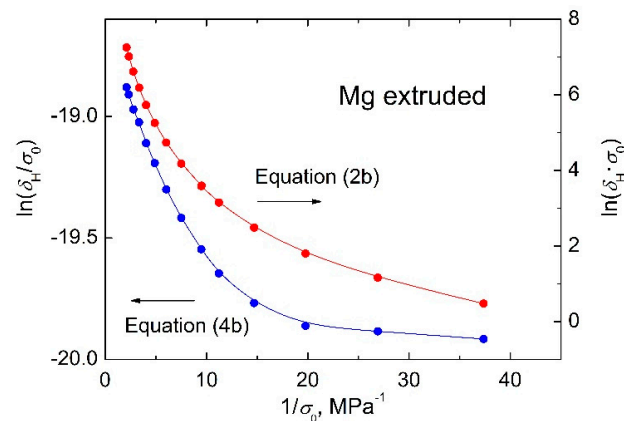


Figure 7. Failed attempts to linearize experimental data using Equation (2b) (right-hand axis) and Equation (4b) (left-hand axis). It can be seen that Equations (2b) and (4b) do not lead to a straightening of the experimental dependences in the coordinates proposed.

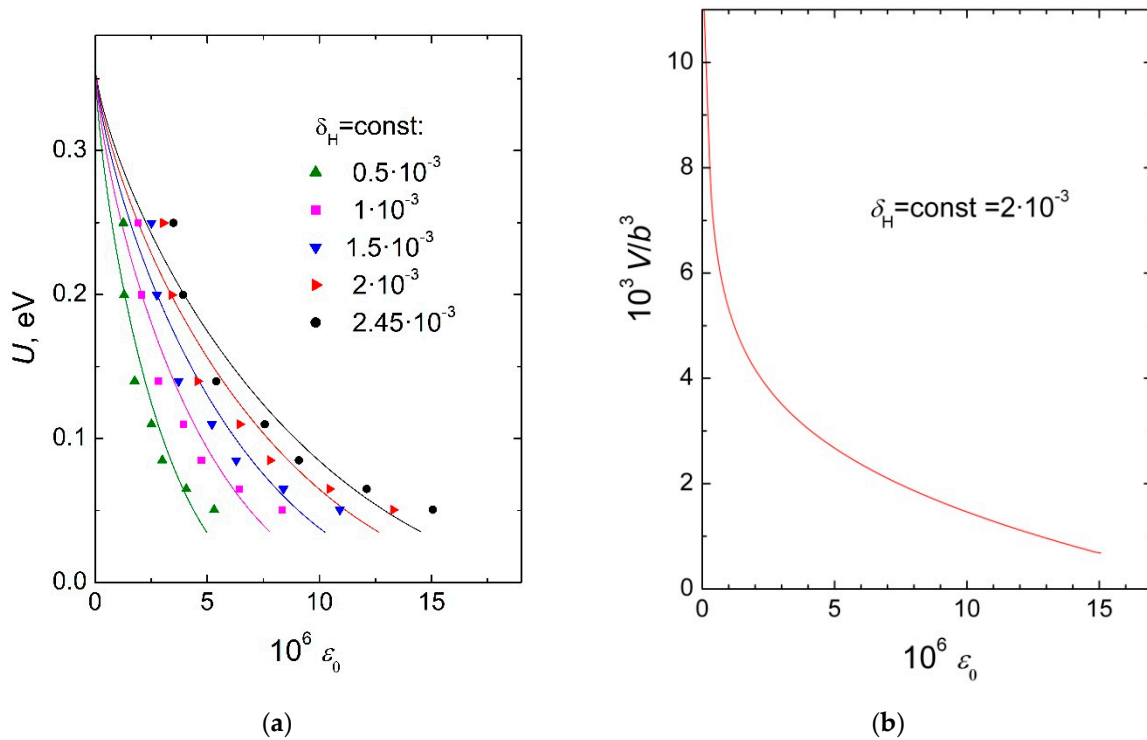


Figure 8. Dependences (a) of the activation energy U on amplitude ε_0 for several sections $\delta_H(T, \varepsilon_0) = \text{const}$ and (b) the activation volume V for the section $\delta_H(T, \varepsilon_0) = 2 \times 10^{-3}$ for the extruded sample.

The sections $\delta_H(T, \varepsilon_0) = \text{const}$, according to [12], can be interpreted as the sections $L_{\min}(T, \varepsilon_0) = \text{const}$, and from the dependence $T(\varepsilon_0)$ along the section $\delta_H = \text{const}$ one can acquire an information on the dependence of the activation energy on the deformation amplitude $U(\varepsilon_0)$ (see Equation (6)). In Figure 6a, the dependences of the activation energy $U(\varepsilon_0)$ for five sections $\delta_H(T, \varepsilon_0) = \text{const}$ are shown. Solid lines in Figure 8a shows the phenomenological stress dependences of the activation energy [14,21]:

$$U(\sigma_0) = U_0 \left(1 - \left(\frac{\sigma_0}{\sigma_M} \right)^p \right)^q, \quad (7)$$

The specific values of p and q are within $0 < p \leq 1$, $1 \leq q \leq 2$ and depend on the size and shape of the potential barriers. They may be determined by fitting Equation (7) to experimental data. To obtain approximate quantitative estimates using (6) and (7), we took the values $\nu_0 \approx 5 \times 10^{10} \text{ s}^{-1}$, $f \approx 7 \times 10^4 \text{ s}^{-1}$, $\sigma_0 \approx E\varepsilon_0$, $E = 44.5 \text{ GPa}$. Fitting Equation (7) to the experimental data in Figure 6a allowed to obtain the values of the binding energy of a dislocation with pinning centers $U_0 = 0.36 \text{ eV}$, $p = 0.78$, $q = 2$. Differentiation of the dependence $U(\sigma_0)$ with respect to σ_0 gives the value of the activation volume $V = \partial U(\sigma_0) / \partial \sigma_0$, the dependence of which on the strain amplitude is shown in Figure 8b for the section $\delta_H(T, \varepsilon_0) = 2 \times 10^{-3}$.

3.2. Temperature Dependences of the Dynamic Young's Modulus

The temperature dependences of the dynamic Young's modulus $E(T)$ in rolled and extruded samples of deformed magnesium of technical purity are shown in Figure 9. The dependences were measured in an amplitude independent region in the temperature range of 51–300 K at a constant amplitude of longitudinal ultrasonic deformation of $\varepsilon_0 = 1 \times 10^{-7}$. When increasing temperature in the range 51–310 K, the dynamic Young's modulus decreased monotonically by a total value of ~10% in both series of samples. It should be noted that the dynamic Young's modulus of extruded samples in the entire investigated temperature range turned out to be almost 5% higher than that of rolled samples. It is worth noting that measured Young's modulus for textured rolled magnesium is in good agreement with theoretical predictions reported for instance in [22]. Indeed, $E = 42.14 \text{ GPa}$ in our rolled samples, $E = 44.20 \text{ GPa}$ in extruded samples for at 300 K and theoretical value is $E_{\text{mean}} = 44.50 \text{ GPa}$. The agreement of Young's modulus values can be considered as ideal since work [22] did not take into account the possible decrease in Young's modulus due to dislocation and texture effects.

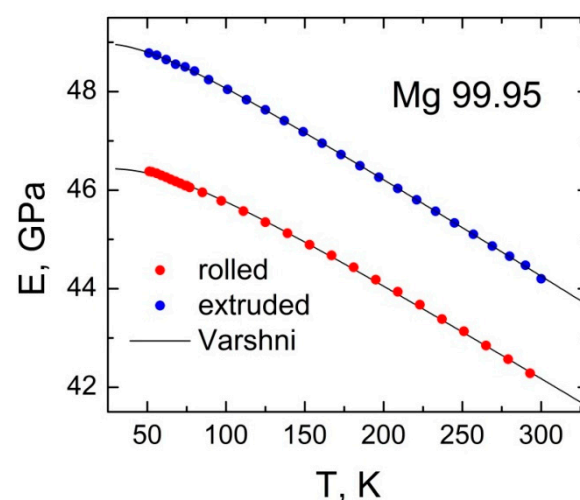


Figure 9. Temperature dependences of the dynamic Young's modulus of rolled and extruded Mg samples. Solid lines show the approximations made using Equation (8).

The theory of the temperature dependence of the elastic moduli was first proposed by Born and Huang [23]. According to [23], this dependence is due to a change in the potential energy of the crystal lattice due to its anharmonicity. In limiting cases, the theory shows that the lattice (phonon) contribution should be proportional to T^4 at very low temperatures and directly proportional to T at high temperatures [23,24]. In perfect metals at low temperatures, an important role is also played by the electronic contribution that is proportional to T^2 [25]. Later, a number of attempts were made to describe the temperature dependence of the elastic moduli using empirical expressions. In particular, Varshni [24] has proposed and theoretically justified an empirical expression suitable for describing the temperature dependences of adiabatic elastic moduli in a wide temperature range for a wide class of crystalline materials:

$$E(T) = E_0 - \frac{a}{\exp(\theta/T) - 1} \quad (8)$$

Here $E(T)$ is the value of the Young's modulus at a given temperature, E_0 is its limiting value at $T \rightarrow 0$ K, θ is the characteristic temperature depending on the material under study, a is a parameter characterizing the joint contribution of thermal excitation of conduction electrons and phonons to the elastic moduli. In crystals with simple phonon spectra, the characteristic temperature θ is close to the Einstein temperature $\theta_E \equiv h\nu_E = 0.75\theta_D$, where h is the Planck constant, ν_E is the frequency of the harmonic oscillator in the Einstein model of solids, θ_D is the Debye temperature. In metals with anomalies in phonon spectra (for example, in the presence of "soft" phonon modes, etc.), the situation is more complicated. Nevertheless, the temperature dependences of the elastic moduli of a large number of crystalline materials can be approximated by Equation (8) with a high degree of accuracy. Table 1 shows the values of the parameters of Equation (8) for describing the temperature dependences of the dynamic Young's modulus $E(T)$ of magnesium polycrystals subjected to plastic deformation by rolling and hot extrusion. In the temperature range $51 \text{ K} < T < 310 \text{ K}$, Equation (8) describes the experimental data with an accuracy no worse than $\pm 0.1\%$.

Table 1. Parameters of approximation of the dynamic Young's modulus temperature dependences by Equation (8) for rolled and extruded Mg samples.

Parameter	Rolled Sample	Extruded Sample
θ , K	185.8	141.3
a , GPa	3.646	2.843
E_0 , GPa	46.440	48.977

It should be noted that the obtained values of the characteristic temperature θ for both groups of samples differ markedly from the Einstein temperature $\theta_E = 0.75 \theta_D = 238 \text{ K}$ (for magnesium $\theta_D = 318 \text{ K}$ [26]). This difference may be due to the fact that Equation (8) was obtained to describe the temperature dependences of the elastic moduli of non-conducting crystals with simple phonon spectra and a small number of crystal structure defects and does not completely correspond to our experimental conditions. Plastic deformation can significantly affect the temperature dependences of Young's modulus $E(T)$ and may lead to the manifestation of quasi-static and dynamic effects [26]. The observed quasi-static excess in Young's modulus by almost 5% over the entire temperature range in the extruded samples can be partially explained by the deformation texture of the extruded samples [2]. The coefficient of elastic anisotropy for magnesium is not so small: the ratio of the largest value of E to the smallest is about 12% [22]. Therefore, the formation of a deformation texture may be considered as a possible reason for the observed difference between the modules in the extruded and rolled samples. An alternative reason for this effect could be difference in values of total dislocation density in the samples after cold and hot working. It is worth noting that the samples were rolled at room temperature, whereas extrusion was carried out at the temperature of $300 \text{ }^\circ\text{C}$ at which it is quite possible

dislocation density reduction due to dynamic recovery processes. This conclusion can be also qualitatively supported by consideration of grain orientation spread (GOS) maps (Figure 10). It can be seen that grains of rolled sample have much wider orientation spread in comparison to extruded sample. This situation is caused by higher dislocation density in the rolled sample.

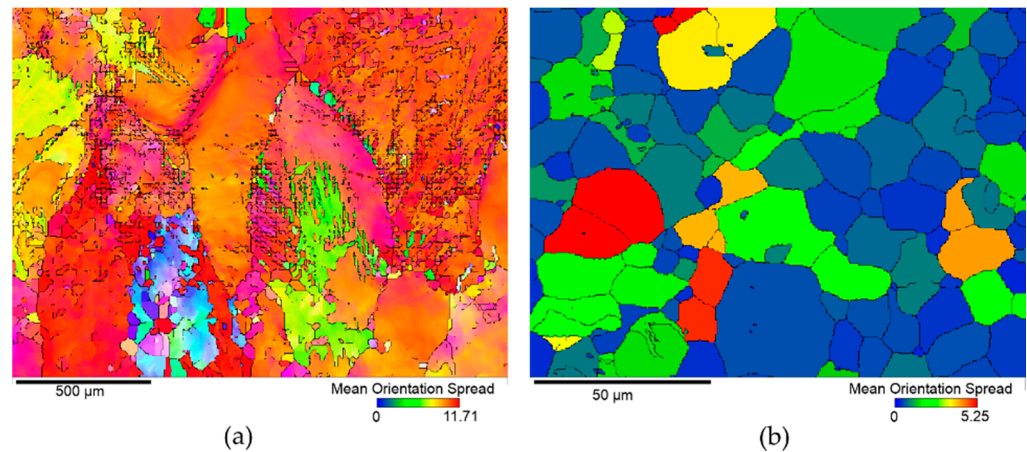


Figure 10. Grain orientation spread (GOS) maps of (a) rolled and (b) extruded sample.

The presence of dislocations in crystals leads to a decrease in the Young's modulus, i.e., a quasi-static modulus defect may be observed, which in the low-frequency limit is determined by the dislocation density Λ and the average length L_c of dislocation segments [14]:

$$(\Delta E/E)_{\text{stat}} \approx \Lambda L_c^2 \quad (9)$$

If we take for the assessment the average length of dislocation segments $L_c = 10^{-6}$ m and assume that it is the same in the rolled and extruded samples (samples are of the same purity), then to ensure the experimentally observed difference in the dynamic Young's moduli of these samples, it is necessary that the dislocation density in the rolled samples should be by $\sim 5 \times 10^{10} \text{ m}^{-2}$ higher than extruded ones. This estimate seems to be quite reasonable in our experimental situation

Dynamic effects associated with thermally activated dynamic relaxation of defect structure elements [1,3,4,27] in the studied temperature range in plastically deformed magnesium polycrystals were not detected.

4. Conclusions

1. In rolled and extruded samples of commercially pure Mg, well-pronounced amplitude dependences of the logarithmic decrement $\delta_H(\varepsilon_0)$ and the relative change in the dynamic Young's modulus $(\Delta E/E)_H(\varepsilon_0)$ are found.
2. With an increase in temperature, the critical amplitude of the beginning of the amplitude dependences ε_{0c} shifts towards lower deformation amplitudes. Above a certain crossover temperature $T_{co} \approx 250$ K for extruded and $T_{co} \approx 180$ K for rolled specimens, this displacement stopped and the curves $\delta_H(\varepsilon_0)$ and $(\Delta E/E)_H(\varepsilon_0)$ began to shift towards higher deformation amplitudes. The data obtained at temperatures above 250 K for extruded specimens and 180 K for rolled specimens may indicate a change in the microscopic mechanism of dislocation motion in deformed Mg at the crossover temperature.
3. The agreement of the experimental data with the Indenbom-Chernov dislocation breakaway theory made it possible to conclude that the dynamic properties of dislocations in technically pure deformed magnesium are largely determined by thermally activated overcoming local pinning centers by dislocations. In the microstrain region, important quantitative characteristics of the interaction of dislocations with pinning

centers (such as the binding energy, strain dependences of the activation energy and the activation volume) have been determined.

4. In the amplitude independent region, the temperature dependences of the dynamic Young's modulus $E(T)$ are obtained. As the temperature rises from 51 to 310 K, Young's modulus decreases by ~10%. In this case, the functional form of the dependences $E(T)$ corresponds to the classical concepts of the effect of thermal excitation of electrons and phonons on the elastic properties of a crystal. Quasi-static increase in Young's modulus by almost 5% over the entire temperature range in the extruded samples may be caused both by formation of a deformation texture and by a difference in total dislocation densities in the samples. Dynamic effects associated with thermally activated dynamic relaxation of defect structure elements (internal friction peaks) in plastically deformed magnesium polycrystals were not detected in the studied temperature range.

Author Contributions: Conceptualization, P.P.-V. and A.O.; investigation, P.P.-V., O.V., L.K. and J.P.; writing—original draft preparation, P.P.-V.; writing—review and editing, P.P.-V. and A.O. All authors have read and agreed to the published version of the manuscript.

Funding: This research was in part funded by bilateral mobility project of Ministry of Education, Youth and Sports of the Czech Republic [grant number 8J19UA037] and Ministry of Education and Science of Ukraine [grant number 0120U103623].

Institutional Review Board Statement: Not applicable.

Informed Consent Statement: Not applicable.

Data Availability Statement: Not applicable.

Conflicts of Interest: The authors declare no conflict of interest.

References

1. Pal-Val, P.P.; Pal-Val, L.N.; Rybalko, A.P.; Vatazhuk, E.N. Change of parameters of the Koiwa-Hasiguti dynamic dislocation relaxation in nanostructured and polycrystalline zirconium after severe plastic deformation and annealing. *Adv. Mater. Sci. Eng.* **2018**, *2018*, 4170187. [[CrossRef](#)]
2. Pal-Val, P.P.; Loginov, Y.N.; Demakov, S.L.; Illarionov, A.G.; Natsik, V.D.; Pal-Val, L.N.; Davydenko, A.A.; Rybalko, A.P. Unusual Young's modulus behavior in ultrafine-grained and microcrystalline copper wires caused by texture changes during processing and annealing. *Mater. Sci. Eng. A* **2014**, *618*, 9–15. [[CrossRef](#)]
3. Golovin, I.S.; Pal-Val, P.P.; Pal-Val, L.N.; Vatazhuk, E.N.; Estrin, Y. The effect of annealing on the internal friction in ECAP-modified ultrafine grained copper. *Solid State Phenom.* **2012**, *184*, 289–294. [[CrossRef](#)]
4. Blanter, M.S.; Golovin, I.S.; Neuhäuser, H.; Sinning, H.-R. *Internal Friction in Metallic Materials: A Handbook*; Springer: Berlin/Heidelberg, Germany, 2007; 539p.
5. Kaminskii, V.V.; Lyubimova, Y.V.; Romanov, A.E. Probing of polycrystalline magnesium at ultrasonic frequencies by mechanical spectroscopy. *Mater. Phys. Mech.* **2020**, *44*, 19–25. [[CrossRef](#)]
6. Trojanová, Z.; Drozd, Z.; Lukáč, P.; Minárik, P.; Džugan, J.; Halmešová, K. Amplitude dependent internal friction in AZ31 alloy sheets submitted to accumulative roll bonding. *Low Temp. Phys.* **2018**, *44*, 966–972. [[CrossRef](#)]
7. Niu, R.; Yan, F.; Wang, Y.; Duan, D.; Yang, X. Effect of Zr content on damping property of Mg–Zr binary alloys. *Mater. Sci. Eng. A* **2018**, *718*, 418–426. [[CrossRef](#)]
8. Uhrčík, M.; Dresslerová, Z.; Soviarová, A.; Palček, P.; Kuchariková, L. Change of internal friction on magnesium alloy with 5.48% Al and 0.813% Zn. *Proc. Eng.* **2017**, *177*, 568–575. [[CrossRef](#)]
9. Watanabe, H.; Sasakura, Y.; Ikeo, N.; Mukai, T. Effect of deformation twins on damping capacity in extruded pure magnesium. *J. Alloy. Compd.* **2015**, *626*, 60–64. [[CrossRef](#)]
10. Koller, M.; Sedlák, P.; Seiner, H.; Ševčík, M.; Landa, M.; Stráská, J.; Janeček, M. An ultrasonic internal friction study of ultrafine-grained AZ31 magnesium alloy. *J. Mater. Sci.* **2015**, *50*, 808–818. [[CrossRef](#)]
11. Granato, A.V.; Lücker, K. The vibrating string model of dislocation damping. In *Physical Acoustics*; Mason, W., Ed.; Academic Press: New York, NY, USA; London, UK, 1966; Volume 4, pp. 225–276.
12. Indenbom, V.L.; Chernov, V.M. Determination of characteristics of the interaction between point defects and dislocations from internal friction experiments. *Phys. Stat. Sol. (a)* **1972**, *14*, 347–354. [[CrossRef](#)]
13. Granato, A.V.; Lücker, K. Temperature dependence of amplitude-dependent dislocation damping. *J. Appl. Phys.* **1981**, *52*, 7136–7142. [[CrossRef](#)]

14. Trojanová, Z.; Drozd, Z.; Lukáč, P.; Džugan, J. Studying the thermally activated processes operating during deformation of hcp and bcc Mg–Li metal-matrix composites. *Metals* **2021**, *11*, 473. [CrossRef]
15. Anes, V.; Lage, Y.E.; Vieira, M.; Maia, N.M.M.; Freitas, M.; Reis, L. Torsional and axial damping properties of the AZ31 B-F magnesium alloy. *Mech. Syst. Sign. Proc.* **2016**, *79*, 112–122. [CrossRef]
16. Cui, Y.; Li, J.; Li, Y.; Koizumi, Y.; Chiba, A. Damping capacity of pre-compressed magnesium alloys after annealing. *Mater. Sci. Eng. A* **2017**, *708*, 104–109. [CrossRef]
17. Janovská, M.; Minárik, P.; Sedlák, P.; Seiner, H.; Knapek, M.; Chmelík, F.; Janeček, M.; Landa, M. Elasticity and internal friction of magnesium alloys at room and elevated temperatures. *J. Mater. Sci.* **2018**, *53*, 8545–8553. [CrossRef]
18. Knapek, M.; Minárik, P.; Trojanová, Z.; Kubásek, J.; Hájek, M.; Šmilauerová, J.; Hofman, D.; Stráská, J. The in-situ mechanical spectroscopy and electric resistance study of WE43 magnesium alloy during aging. *J. Alloy. Compd.* **2018**, *743*, 646–653. [CrossRef]
19. Wang, Y.N.; Huang, J.C. Texture analysis in hexagonal materials. *Mater. Chem. Phys.* **2003**, *81*, 11–26. [CrossRef]
20. Natsik, V.D.; Pal-Val, P.P.; Smirnov, S.N. Theory of a compound piezoelectric vibrator. *Acoust. Phys.* **1998**, *44*, 553–560.
21. Kocks, U.F.; Argon, A.S.; Ashby, M.F. Thermodynamics and Kinetics of Slip. In *Progress in Materials Science 19*; Pergamon Press: Oxford/Edinburg, UK; New York, NY, USA; Toronto, ON, Canada, 1975.
22. Tromans, D. Elastic anisotropy of hcp metal crystals and polycrystals. *Int. J. Res. Rev. Appl. Sci.* **2011**, *6*, 462–483. Available online: https://www.arpapress.com/Volumes/Vol6Issue4/IJRRAS_6_4_14.pdf (accessed on 17 October 2021).
23. Born, M.; Huang, K. *Dynamical Theory of Crystal Lattices*; Oxford University Press: London, UK, 1954.
24. Varshni, Y.P. Temperature dependence of the elastic constants. *Phys. Rev. B* **1970**, *2*, 3952–3958. [CrossRef]
25. Alers, G.A. The measurement of very small sound velocity changes and their use in the study of solids. In *Physical Acoustics*; Mason, W., Ed.; Academic Press: New York, NY, USA; London, UK, 1966; Volume 4, pp. 277–296.
26. Girifalco, L.A. *Statistical Mechanics of Solids*; Oxford University Press: New York, NY, USA, 2000; 519p.
27. Vatazhuk, E.N.; Pal-Val, P.P.; Natsik, V.D.; Pal-Val, L.N.; Tikhonovsky, M.A.; Velikodny, A.N.; Khaimovich, P.A. Low-temperature acoustic properties of nanostructured zirconium obtained by intensive plastic deformation. *Low Temp. Phys.* **2011**, *37*, 169–176. [CrossRef]